Designing a stronger interface through graded structures in amorphous/nanocrystalline ZrCu/Cu multilayered films

2016 Nanotechnology 27 225701

(http://iopscience.iop.org/0957-4484/27/22/225701)

IOP Publishing Nanotechnology
Nanotechnology 27 (2016) 225701 (7pp) doi:10.1088/0957-4484/27/22/225701

Designing a stronger interface through graded structures in amorphous/nanocrystalline ZrCu/Cu multilayered films

C H Chang[1], C H Hsieh[1], J C Huang[1], C Wang[2], Y C Liao[2], C H Hsueh[2], X H Du[1], Z K Wang[1] and X Wang[1]

[1] Department of Materials and Optoelectronic Science, National Sun Yat-Sen University, Kaohsiung, Taiwan 804, Republic of China
[2] Department of Materials Science and Engineering, National Taiwan University, Taipei, Taiwan 106, Republic of China

E-mail: jacobc@mail.nsysu.edu.tw

Received 10 February 2016, revised 22 March 2016
Accepted for publication 23 March 2016
Published 22 April 2016

Abstract

Many multilayered nano-structures appear to fail due to brittle matter along the interfaces. In order to toughen them, in this study, the microstructure and interface strength of multilayered thin films consisting of amorphous ZrCu and nanocrystalline Cu (with sharp or graded interfaces) are examined and analyzed. The interface possesses a gradient nature in terms of composition, nanocrystalline phase size and volume fraction. The bending results extracted from the nano-scaled cantilever bending samples demonstrate that multilayered films with graded interfaces would have a much higher interface bending strength/strain/modulus, and an overall improvement upgrade of more than 50%. The simple graded interface design of multilayered thin films with improved mechanical properties can offer much more promising performance in structural and functional applications for MEMS or optical coating.

Keywords: metallic glass, nanocrystalline phase, graded structure, interface, cantilever bending

(Some figures may appear in colour only in the online journal)

1. Introduction

Bulk metallic glasses (BMGs) were developed decades ago [1], and because of their unique properties, such as high levels of hardness, high strength, good corrosion resistance and great shaping and forming ability in the liquid state, etc, they have attracted much attention [2–6]. Recently, thin-film metallic glasses (TFMGs) have also been researched and it might become possible to apply them to many microelectromechanical system (MEMS) devices [7–10]. However, their brittle nature at room temperature appears to be a drawback in the application of these glasses [11, 12]. To solve this problem, the concept of a composite consisting of MG and nanocrystalline (NC) dual phases has been developed. This involves incorporating uniformly dispersed ductile nanocrystalline metal particulate phases to the amorphous matrix, or by forming a multilayered film structure to improve its mechanical properties [13–16].

Nieh *et al* examined amorphous/crystalline ZrCu/Cu nano-laminates and achieved high strength and good ductility [15]. According to Liu *et al*, when the thickness of each ZrCu/Cu layer is lowered to 100 nm, the multilayered films exhibit the best plasticity [17].

Even though amorphous/nanocrystalline multilayered thin films could improve plasticity, they might be subject to interface debonding due to the mismatch in modulus and strength between neighboring layers [18]. When a crack propagates within multilayered films, it could either penetrate the interface or deflect along the debonded interface [19, 20]. According to the numerical calculation by Hsueh [21], the graded layer could decrease the lattice mismatch and mitigate the mismatch strain between two different materials. Also,

from the simulated results, the graded structure could change the stress distribution and then improve the mechanical properties [22, 23]. Inspired by such results, to decrease the modulus/strength mismatch, the design of a graded interface region in terms of composition, grain size or amorphous degree might be helpful.

Since the 1990s, multilayered materials with graded composition structures—often called functional graded materials (FGM)—have been widely investigated for alloys, ceramics, or metal/ceramic composites, such as W/Cu [24], ZrO_2/TiO_2 [25], AlN/GaN [26], and Ni/YSZ [27]. In 2011, Wang *et al* adopted surface mechanical attrition treatment (SMAT) on pure Cu to produce graded grain-sized structures [28]. At the same time, Fang *et al* presented Cu thin films with graded grain sizes that could achieve high yield stress and promising elongation under tensile testing [29]. Moreover, the Zr50Cu50/Cu amorphous/nanocrystalline multilayered films with graded interfaces, reported by Pei *et al* [30], exhibited a Young's modulus of ~100 GPa, a yield stress of ~800 MPa and a tensile strain to fracture of ~2.3% —all greater than the multilayered films with sharp interfaces. According to these studies, it is essential to explore the detailed microstructure and interface strength for such sharp and graded interfaces further [30].

2. Experimental procedures

The multilayered films were deposited on a silicon wafer using a direct current (DC) magnetron sputtering system. In the sputtering system, a $Zr_{50}Cu_{50}$ (in atomic percent, at%) alloy target and a pure Cu target were used. The formation of the graded region in the Zr–Cu binary system is based on the huge composition window (from about Zr-20 at% Cu to Zr-80 at% Cu), which forms the amorphous structure by sputtering. When the Cu and Zr contents exceed the ceiling, the remaining contents can precipitate the crystalline phase within the amorphous matrix, forming a composite structure [31]. To fabricate the ZrCu/Cu multilayered thin films with graded or sharp interfaces, the power of the $Zr_{50}Cu_{50}$ and Cu guns was adjusted between 50–200 W and 50–150 W, respectively. The resulting ZrCu layers are designed to be fully amorphous and the Cu layers have a nanocrystalline structure. The operation of the gradual power change is quite simple and the current-graded interface design can easily be applied to large-scale film industries. The graded regions can vary from 20 to 200 nm thick by using different time intervals to increase or decrease the power of the targets. Within the graded interface region, the ZrCu amorphous phase and the crystalline Cu phase vary their partitions according to the adjustments to the target power. The length of the graded interface region is thus determined by the time interval length for the relative power change. This paper adopts 50 and 100 nm thicknesses for comparison with the sharp interfaces. For simplicity, the ZrCu/Cu multilayered thin-film samples with sharp and graded interfaces are termed as ZCC-S, ZCC-G50 and ZCC-G100, respectively.

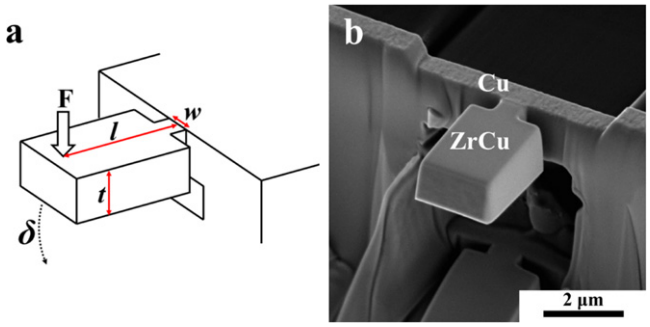

Figure 1. Illustration of the T-shaped cantilever bending sample: (a) schematic drawing with the dimensions of bending length *l*, width of the narrow section *w*, and thickness *t*, and (b) SEM micrograph. The interface region is located within the narrow *w* section.

The structure and the element distribution characteristics of these thin films were confirmed using an FEI Tecnai field-emission transmission electron microscope (TEM) with an energy dispersive x-ray spectrometer (EDS), and scanning transmission electron microscope (STEM) with a high angle annular dark field detector (HAADF). The cross-section TEM foils were fabricated using the SEIKO SMI3050 dual-focus ion beam (FIB) system.

In order to explore the mechanical strength of the graded or sharp interface region, we simplified the multilayered films into a bilayered structure consisting of only the ZrCu metallic glassy layer and the Cu nanocrsytalline layer. The deposited bottom layer facing the Si wafer is nanocrystalline Cu, about 600–700 nm thick, and the top surface layer is the ZrCu metallic glass, about 3000–3500 nm thick. The above thickness was intentionally designed to fit the subsequent bending test samples. Recently, bending tests in the micro- and nano-scale have been widely developed [32–35]. In this study, the sputtered Si/Cu/ZrCu films were formed into cantilever bending test samples using the FIB system, and tested by a Hysitron PI 85 PicoIndenter installed in the scanning electron microscope (SEM) in the *in situ* video-camera mode. The design of the cantilever bending test samples is presented in figure 1. The bending length *l*, the width of the narrow section *w*, and the thickness *t* are carefully measured using an SEM and are listed in table 1. The reason for designing a narrow section was to ensure that failure would occur in the section where the sharp or graded interface was intentionally located. Multiple tests were conducted and the average is presented in this paper. To calculate the bending stress and strain, precise measurements of length, width and thickness are required for each sample.

The current study adopts bending tests instead of tension or compression testing. This is mainly based on the consideration that the graded interface region is rather thin, making the design of tensile or compression samples with a gauge length of about 100 nm rather difficult. A bending sample can possess a large dimension for loading, and the

Table 1. Experimental parameters for the ZCC-G0, ZCC-G50 and ZCC-G100 samples under bending testing.

	Maximum load (μN)	Bending length (l: μm)	Width of the narrow section (w: μm)	Cantilever thickness (t: μm)
ZCC-G0	321	2.49	0.89	1.65
ZCC-G50	220	2.98	0.66	1.50
ZCC-G100	290	3.30	0.64	1.74

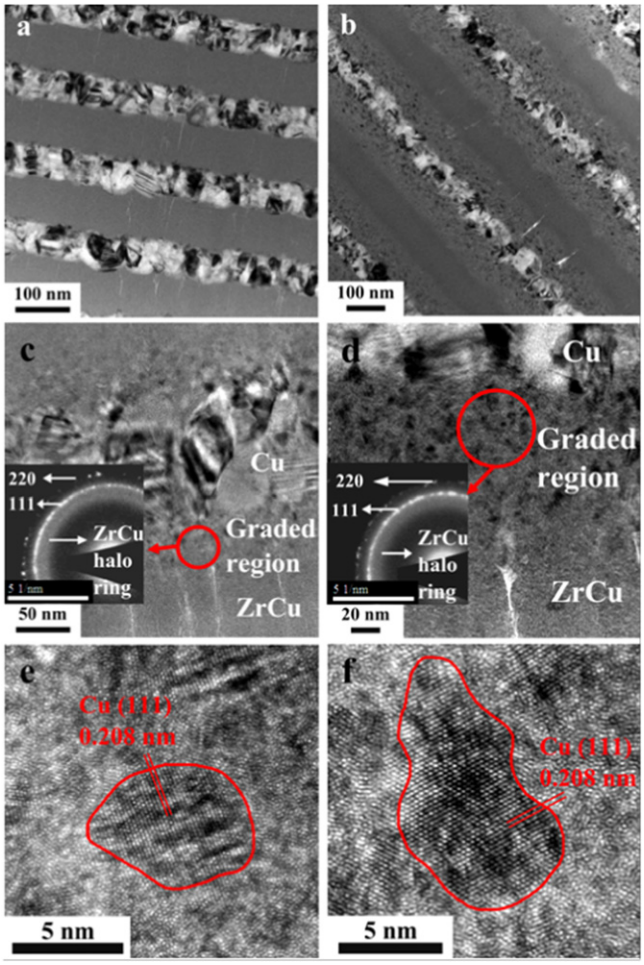

Figure 2. TEM cross-sectional micrographs of multilayered ZrCu/Cu films: (a) ZCC-S with sharp interfaces, (b) ZCC-G100 with graded interfaces. The enlarged bright-field images for (c) ZCC-G50 and (d) ZCC-G100, both with the inserted diffraction patterns, (e) high-resolution lattice image for the Cu particle near the ZrCu fully amorphous layer, and (f) the Cu particle near the Cu nanocrystalline layer, taken from the ZCC-G100 sample.

properties of the weakest interface region, sharp or graded, can be more easily evaluated.

3. Results and discussion

The cross-sectional TEM bright-field images of the multilayered ZrCu/Cu films with sharp and graded interfaces—or ZCC-S and ZCC-G100—are presented in figures 2(a) and (b), respectively. By using different power-changing time intervals in the sputtering, graded regions of two different thicknesses can be fabricated between the ZrCu and Cu layer, as shown in figures 2(c) and (d). It can be seen that the thickness of each layer is about 100 nm for all the ZrCu and Cu multilayers. In the enlarged bright-field images in figures 2(c) and (d), the graded region is about 50 and 100 nm for the ZCC-G50 and ZCC-G100, respectively. The nano-beam diffraction pattern taken from the graded region can be seen in the inset of figures 2(c) and (d). The diffraction pattern contains the halo diffuse ring brought about by the amorphous ZrCu matrix and the sharper discrete reflections (as discrete ring patterns) referred to the {111} and {220} planes of the pure Cu nanoparticles. Furthermore, the high-resolution TEM fringe image, taken by the interference between the central beam and {111} the reflection beam, is shown in figures 2(e) and (f). The spacing of the lattice fringes in figures 2(e) and (f) is ~0.208 nm, consistent with the d-spacing of Cu {111} and the {111} reflection in the diffraction pattern. From the TEM bright-field images in figures 2(c) and (d), the Cu particles are measured and averaged to be about 2–10 nm in the two ZCC-G samples. The Cu particle size appears to be smaller (~2 nm) and the particle amount appears to be lower in volume fraction near the ZrCu fully amorphous layer, and they become larger (~10 nm) and appear in greater quantity near the Cu nanocrystalline layer.

By taking advantage of the image contrast of the HAADF originating from the different atomic weights of Zr (91.2) and Cu (63.5), the HAADF STEM can reveal the local concentration changes from the fully amorphous ZrCu layer, to the graded regime of the ZrCu embedded with Cu nanoparticles, and then to the nanocrystalline Cu layer. Along the direction of the arrows in figures 3(a) and (b) of the HAADF images, changes in the level of gray from the darker ZrCu all the way to the brighter Cu are evident, revealing the gradual concentration change in both ZCC-G50 and ZCC-G100. The semi-quantitative measurement from the TEM nano-beam EDS point analysis (as shown in figure 3(c)) reveals that the amorphous ZrCu layer, with about 50 at% Zr and 50 at% Cu, gradually increases its Cu content to 100% when the scan moves across the graded interface region and finally ends up at the pure Cu nanocrystalline layer. Note that the concentration change of ZCC-G50 is sharper than that of ZCC-G100.

In order to assess the role played by the sharp or graded region in terms of mechanical response, we fabricated a T-shaped cantilever at the edge of the sample using the FIB system; the interface or the graded region was located at the narrow section of the cantilever. Although tensile testing is the simplest, most accurate way of understanding the mechanical properties of materials, in our experiment, based on the rule of mixture [30], the strength of the graded region should be greater than that of the Cu layer. Thus, under

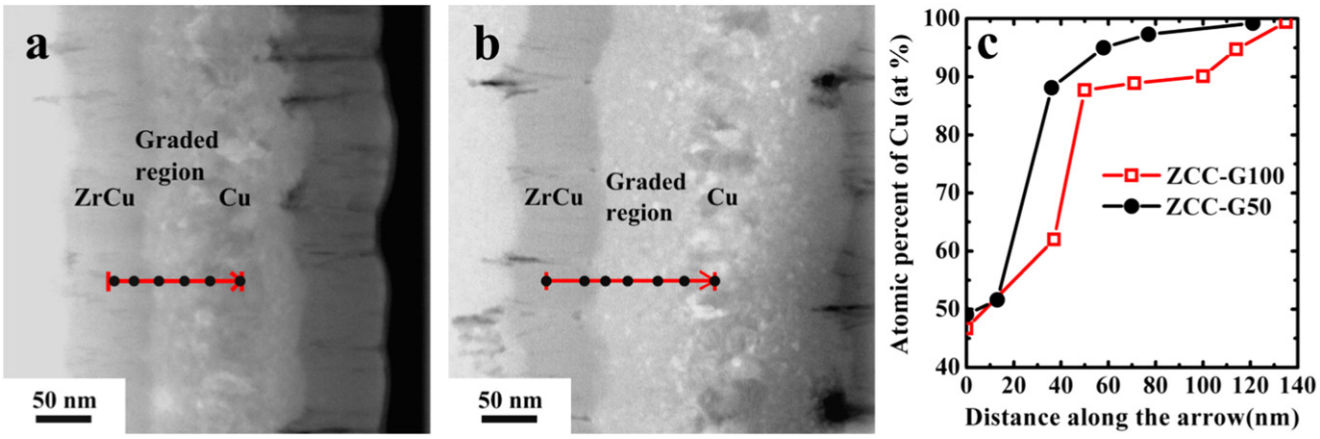

Figure 3. TEM HAADF image of (a) ZCC-G50, and (b) ZCC-G100, showing the left-hand side of the amorphous ZrCu layer, followed by the graded region and then the nanocrystalline Cu layer; (c) the TEM nano-beam EDS points analysis measurement along the red line in (a) and (b) from the left-hand side, demonstrating the gradual increase in Cu content.

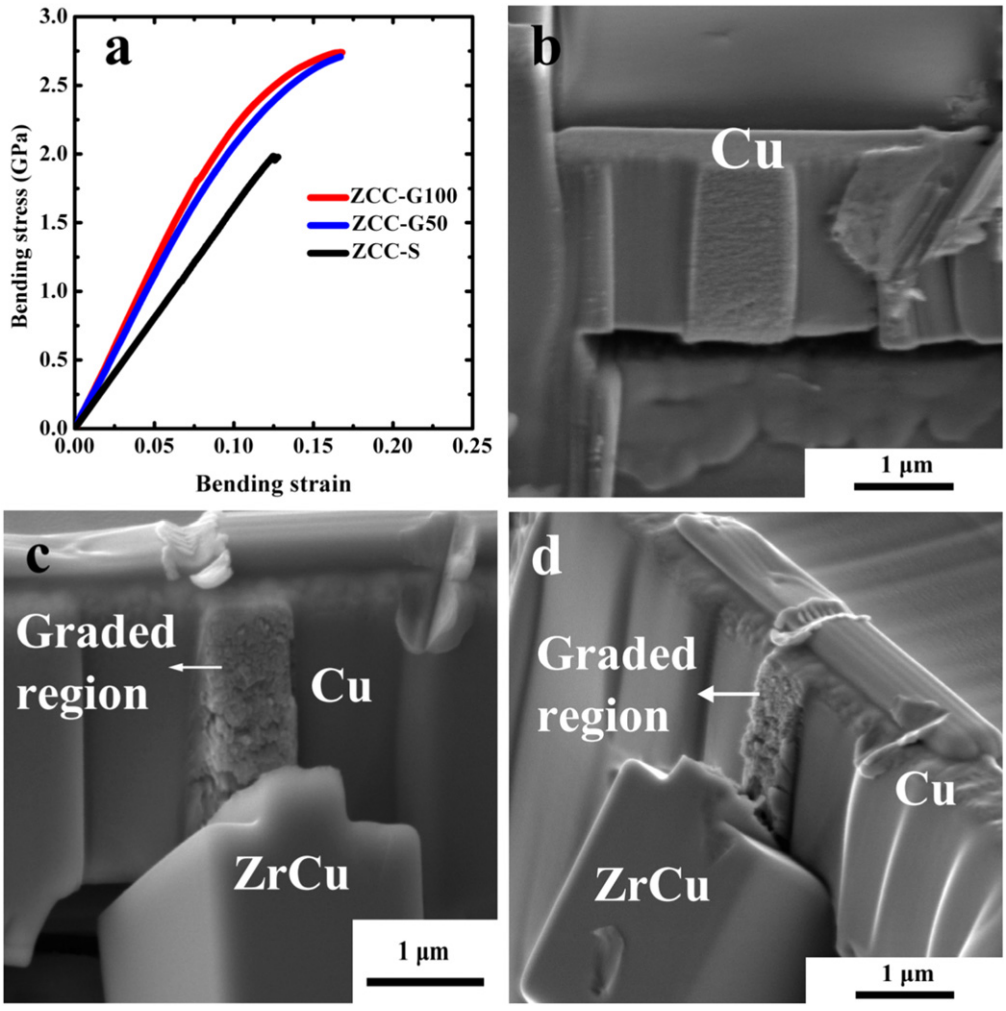

Figure 4. (a) Representative bending stress and strain curves for the ZCC-S, ZCC-G50 and ZCC-G100 samples. The SEM micrographs of (b) ZCC-S with a smooth and brittle fracture surface, and (c) and (d) ZCC-G100 with a rough and ductile fracture surface.

tension, the tension deformation would concentrate entirely within the Cu layer contribution, leaving the graded region and the ZrCu layer undeformed. It is also difficult to fabricate a tension gauge consisting solely of the graded region (only 50–100 nm in length) using the FIB system—there would be too many artificial defects induced by Ga+ ion etching during the FIB processing. It follows that we adopt the bending test to extract the sharp and graded interface properties.

The bending stress for such cantilever samples can be calculated by [36, 37]

$$\sigma = \frac{6Fl}{wt^2}, \quad (1)$$

where F is the applied load. Meanwhile, the bending strain can be calculated by [36, 37]

$$\varepsilon = \frac{3\delta t}{2l^2}, \quad (2)$$

where δ is the deflection depth of the cantilever.

First, for the ZCC-S samples, the representative bending stress versus strain curve is presented in figure 4(a). The failure process was video-taped and the selected fracture surface is shown in figure 4(b). The crack was seen to initiate from the top surface of the narrow w section along the ZrCu/Cu sharp interface, when the load (or stress) reached the peak of the curve. The crack proceeded in a catastrophic manner, showing a rather brittle and smooth fracture surface along the sharp ZrCu/Cu interface. According to equation (1), the average bending fracture stress, or the interface bending stress, for the ZCC-S samples is 1.9 ± 0.1 GPa. The bending strain is about $11 \pm 1\%$. In addition, the bending modulus E_b and bending angle θ are 15 ± 1 GPa and $7 \pm 1^\circ$, respectively.

The ZCC-G50 and ZCC-G100 samples were tested in parallel. The representative bending stress versus strain curve is also presented in figure 4(a) for comparison. Figures 4(c) and (d) are two selected micrographs illustrating the rough fracture surface. The crack also started from the top surface of the narrow w section. However, during crack propagation, it proceeded in a zig-zag manner from the top to the bottom surface along the graded interface region. Sometimes, the major crack path would form branches along the horizontal or inclined direction within the graded region, or even into the Cu layer. It is apparent that the failure mode was much more ductile in nature, as evident from the bending stress and strain curve with plastic deformation shown in figure 4(a). The exact zig-zag or branching deflection of the crack propagation in a fine scale of a few nanometers is difficult to trace clearly with the *in situ* SEM video due to the instrument's resolution limit. By comparing the *ex situ* SEM images of the fracture surfaces in the samples with the sharp or graded interface regions, it is postulated that the uneven fracture surfaces in the graded samples are caused by the uniform dispersed nanocrystalline Cu particles in the fully amorphous ZrCu matrix.

According to equation (1), the average bending yield stress for the ZCC-G50 or ZCC-G100 sample is about 2.4 ± 0.1 GPa, and the fracture stress, or the interface bending stress, is 2.8 ± 0.2 GPa. The bending strain is about $18 \pm 1\%$ (including about 6%–8% plastic bending strain). In addition, the bending modulus E_b and bending angle θ are 18 ± 1 GPa and $11 \pm 1^\circ$, respectively.

Based on the above results, it is demonstrated that there is no significant difference between the ZrCu/Cu bilayered thin film in the 50 and 100 nm graded region: both reveal the ability to deflect crack propagation, inducing branching and plastic deformation. The more significant finding is the increase of interface bending stress from 1.9 up to 2.8 GPa, an increment of nearly 50%. This significant increment might have been brought about by the strengthening of the interface region due to the dispersal of Cu particles in the amorphous ZrCu matrix, as can be predicted by the rule of mixture [30]. Furthermore, the interface bending strain would increase from 11% to 18% and the bending modulus from 15 to 18 GPa, increments of 64% and 20%, respectively. The concurrent increases in bending stress, bending strain, bending modulus and bending angle demonstrate the overall upgraded mechanical performance brought about by the incorporation of graded interfaces. It is necessary to note that the current bending strain is not really equal to the tensile ductility, but is more related to resistance against the propagation of the first crack originating in the top surface. It is more like a bending toughness concept.

The underlying reasons for providing such an overall improvement originate from the avoidance of sharp interfaces with a sharp modulus and strength mismatch between the two neighboring thin layers. The graded interface region can replace the sharp mismatch in continuous compositional, structural, and property gradients which would avoid the sharp modulus and strength mismatch between the two neighboring materials. The bonding therefore becomes much more compatible, significantly reducing the debonding drawback. The whole graded region would result in a Young's modulus gradient, thus avoiding a sudden modulus drop at the interface. The current-graded design proves to be a simple and promising route towards improving multilayered thin films with mismatched layers.

In addition, the toughening mechanism can be rationalized by previous reports on the metallic glass composite idea [38–47]. For the ZrCu amorphous layer with ductile Cu soft elastic/plastic inhomogeneities in a metallic glass matrix, it can initiate more local shear banding around the inhomogeneities [45], and can match the microstructural length scales to the characteristic length scale R_P (for the plastic shielding of an opening crack tip) to limit shear band extension, suppress the shear band opening, and avoid crack development [45]. In accordance with the above arguments, the ZrCu metallic glass matrix in the graded region itself can be toughened by the Cu particles.

Meanwhile, the embedded Cu nanoparticles can increase the strength of the interface region via the precipitation strengthening mechanism. Cu nano precipitates are formed during sputtering due to excess Cu content. This is different from controlled crystallization via thermal annealing treatment from the fully amorphous matrix [48]. The graded region should be stronger than the Cu layer. Among the three regions (the ZrCu MG layer, the graded region, and the Cu layer), the 'softest' and thus the part to deform most easily under bending is the nanocrystalline Cu layer. Under bending, the characteristic dimension R_p of a crack tip 'plastic zone' for the nanocrystalline Cu layer (about ~1 mm) would significantly exceed the sample thickness t of 2000 ± 200 nm. Therefore, during the bending plastic deformation process, a large number of dislocations would be activated in the nanocrystalline Cu layer. For the sample with a sharp

interface, the dislocation pile-up would induce stress concentration at the sharp interface, leading to premature brittle fracture. However, for the sample with the graded interface, fortunately, the already toughened graded region (by the deformable Cu particles) can act as a high-capacity sink for the coming dislocations due to its favorable slip transfer characteristics. In such a way, the dislocation slip mechanism in the nanocrystalline Cu layer can be modulated by the nano-scale graded region; thus, the propagation of brittle cracks can be prevented. In addition, the suppression of such cracks through modulus gradients would help prevent the introduction of residual bending stresses in the bulk. For the above reasons, the T-shaped sample including the graded region exhibits improved bending plastic strain, characterized by the formation of a rough fracture surface which is composed of lots of 'ductile voids', as shown in figure 4.

These mechanical property improvements potentially make multilayered TFMGs more promising for applications in MEMS or optical coating. Some applications involving coating on a hard substrate Si or soft substrate PET have already been tried along these lines in order to bring about an upgrade in the performance of their electrical or optical characteristics [49–53].

4. Conclusion

The microstructure and interface response of multilayered thin films consisting of amorphous ZrCu and nanocrystalline Cu, with sharp or graded interfaces, have been explored and compared.

1. The graded interfaces can be fabricated simply by adjusting the sputter power, resulting in gradient regions varying in thickness from 20 to 200 nm.
2. The interface possesses a gradient nature in terms of composition, nanocrystalline phase size and volume fraction.
3. The bending results extracted from the nano-scaled cantilever bending samples demonstrate that multilayered films with graded interfaces would inherit a much higher interface strength/strain/modulus, with an overall improvement upgrade of more than 50%.

The current-graded design proves to be a simple and promising route towards improving multilayered thin films with mismatched layers.

Acknowledgments

The authors gratefully acknowledge sponsorship from the Ministry of Science and Technology of Taiwan, ROC, under the project no. MOST 102-2221-E-110-025-MY3. The authors would also like to thank Prof. T G Nieh for useful technical discussion.

References

[1] Klement W, Willens R H and Duwez P 1960 Non-crystalline structure in solidified gold–silicon alloys *Nature* **187** 869–70
[2] Schroers J 2010 Processing of bulk metallic glass *Adv. Mater.* **22** 1566–97
[3] Johnson W L 1999 Bulk glass-forming metallic alloys: science and technology *MRS Bull.* **24** 42–56
[4] Inoue A 2000 Stabilization of metallic supercooled liquid and bulk amorphous alloys *Acta Mater.* **48** 279–306
[5] Chen N, Louzguine-Luzgin D V, Xie G Q, Sharma P, Perepezko J H, Esashi M, Yavari A R and Inoue A 2013 Structural investigation and mechanical properties of a representative of a new class of materials: nanograined metallic glasses *Nanotechnology* **24** 045610
[6] Kumar G, Blawzdziewicz J and Schroers J 2013 Controllable nanoimprinting of metallic glasses: effect of pressure and interfacial properties *Nanotechnology* **24** 105301
[7] Yu H B, Luo Y and Samwer K 2013 Ultrastable metallic glass *Adv. Mater.* **25** 5904–8
[8] Chen C J, Huang J C, Chou H S, Lai Y H, Chang L W, Du X H, Chu J P and Nieh T G 2009 On the amorphous and nanocrystalline Zr-Cu and Zr-Ti co-sputtered thin films *J. Alloys Compd.* **483** 337–40
[9] Hasan M, Schroers J and Kumar G 2015 Functionalization of metallic glasses through hierarchical patterning *Nano Lett.* **15** 963–8
[10] Sharma P, Kaushik N, Kimura H, Saotome Y and Inoue A 2007 Nano-fabrication with metallic glass—an exotic material for nano-electromechanical systems *Nanotechnology* **18** 035302
[11] Liu C T, Heatherly L, Horton J A, Easton D S, Carmichael C A, Wright J L, Schneibel J H, Yoo M H, Chen C H and Inoue A 1998 Test environments and mechanical properties of Zr-base bulk amorphous alloys *Metall. Mater. Trans.* A **29** 1811–20
[12] Li H, Fan C, Tao K, Choo H and Liaw P K 2006 Compressive behavior of a Zr-based metallic glass at cryogenic temperatures *Adv. Mater.* **18** 752–4
[13] Kim J Y, Jang D and Greer J R 2011 Nanolaminates utilizing size-dependent homogeneous plasticity of metallic glasses *Adv. Funct. Mater.* **21** 4550–4
[14] Lee C J, Lin H K, Huang J C and Kuan S Y 2011 Tension behavior of free-standing amorphous film and amorphous-crystalline nanolaminates in submicron scale *Scr. Mater.* **65** 695–8
[15] Nieh T G, Barbee T W and Wadsworth J 1999 Tensile properties of a free-standing Cu/Zr nanolaminate (or compositionally-modulated thin film) *Scr. Mater.* **41** 929–35
[16] Donohue A, Spaepen F, Hoagland R G and Misra A 2007 Suppression of the shear band instability during plastic flow of nanometer-scale confined metallic glasses *Appl. Phys. Lett.* **91** 2013–6
[17] Liu M C, Huang J C, Chou H S, Lai Y H, Lee C J and Nieh T G 2009 A nanoscaled underlayer confinement approach for achieving extraordinarily plastic amorphous thin film *Scr. Mater.* **61** 840–3
[18] Launey M E, Hofmann D C, Johnson W L and Ritchie R O 2009 Solution to the problem of the poor cyclic fatigue resistance of bulk metallic glasses *Proc. Natl Acad. Sci. USA* **106** 4986–91
[19] Dauskardt R H, Lane M, Ma Q and Krishna N 1998 Adhesion and debonding of multi-layer thin film structures *Eng. Fract. Mech.* **61** 141–62
[20] Liu M C, Huang J C, Fong Y T, Ju S P, Du X H, Pei H J and Nieh T G 2013 Assessing the interfacial strength of an amorphous-crystalline interface *Acta Mater.* **61** 3304–13
[21] Hsueh C H 2003 *J. Cryst. Growth* **258** 302–9

[22] Bourada M, Kaci A, Houari M S A and Tounsi A 2015 A new simple shear and normal deformations theory for functionally graded beams *Steel Compos. Struct.* **18** 409–23
[23] Mahi A, Adda Bedia E A and Tounsi A 2015 A new hyperbolic shear deformation theory for bending and free vibration analysis of isotropic, functionally graded, sandwich and laminated composite plates *Appl. Math. Model.* **39** 2489–508
[24] Meng Y, Shen Y, Chen C, Li Y and Feng X 2014 Effects of Cu content and mechanical alloying parameters on the preparation of W-Cu composite coatings on copper substrate *J. Alloys Compd.* **585** 368–75
[25] Huang J, Ichinose I, Kunitake T and Nakao A 2002 Zirconia-Titania nanofilm with composition gradient *Nano Lett.* **2** 669–72
[26] Raghavan S and Redwing J M 2005 Growth stresses and cracking in GaN films on (111) Si grown by metal-organic chemical-vapor deposition: I. AlN buffer layers *J. Appl. Phys.* **98** 023515
[27] Sengupta P, Rogalla D, Becker H W, Dey G K and Chakraborty S 2011 Development of graded Ni-YSZ composite coating on Alloy 690 by pulsed laser deposition technique to reduce hazardous metallic nuclear waste inventory *J. Hazard. Mater.* **192** 208–21
[28] Wang Z B, Lu K, Wilde G and Divinski S V 2010 Interfacial diffusion in Cu with a gradient nanostructured surface layer *Acta Mater.* **58** 2376–86
[29] Fang T H, Li W L, Tao N R and Lu K 2011 Revealing extraordinary intrinsic tensile plasticity in gradient nano-grained copper *Science* **331** 1587–90
[30] Pei H J, Kuan S Y, Liu M C and Huang J C 2012 Tensile behavior of amorphous/nanocrystalline ZrCu/Cu multilayered films with graded interfaces *Intermetallics* **31** 191–5
[31] Xie L, Brault P, Thomann A and Bedra L 2013 Molecular dynamic simulation of binary Zr_xCu_{100-x} metallic glass thin film growth *Appl. Surf. Sci.* **274** 164–70
[32] Allison P G, Moser R D, Schirer J P, Martens R L, Jordon J B and Chandler M Q 2014 *Mater. Lett.* **131** 313–6
[33] Kamiya S, Furuta H and Omiya M 2007 *Surf. Coatings Technol.* **202** 1084–8
[34] Sumigawa T, Shishido T, Murakami T and Kitamura T 2010 *Mater. Sci. Eng.* A **527** 4796–803
[35] Kawai E, Sanada K, Sumigawa T and Kitamura T 2014 *Eng. Fract. Mech.* **120** 60–6
[36] Weihs T P, Hong S, Bravman J C and Nix W D 1988 Mechanical deflection of cantilever microbeams: A new technique for testing the mechanical properties of thin films *J. Mater. Res.* **3** 931–42
[37] Yang H J, Pei Y T, Song G M and De Hosson J T M 2013 Healing performance of Ti 2AlC ceramic studied with *in situ* microcantilever bending *J. Eur. Ceram. Soc.* **33** 383–91
[38] Szuecs F, Kim C P and Johnson W L 2001 *Acta Mater.* **49** 1507–13
[39] Fan C, Ott R T and Hufnagel T C 2002 *Appl. Phys. Lett.* **81** 1020
[40] Kühn U, Eckert J, Mattern N and Schultz L 2002 *Appl. Phys. Lett.* **80** 2478
[41] Kato H, Yubuta K, Louzguine D V, Inoue A and Kim H S 2004 *Scr. Mater.* **51** 577–81
[42] Lim H K, Park E S, Park J S, Kim W T and Kim D H 2005 *J. Mater. Sci.* **40** 6127–30
[43] Fu H, Zhang H, Wang H, Zhang Q and Hu Z 2005 *Scr. Mater.* **52** 669–73
[44] Xu Y K, Ma H, Xu J and Ma E 2005 *Acta Mater.* **53** 1857–66
[45] Hofmann D C, Suh J Y, Wiest A, Duan G, Lind M L, Demetriou M D and Johnson W L 2008 Designing metallic glass matrix composites with high toughness and tensile ductility *Nature* **451** 1085–9
[46] Jang J S C, Ciou J Y, Hung T H, Huang J C and Du X H 2008 Enhanced mechanical performance of Mg metallic glass with porous Mo particles *Appl. Phys. Lett.* **92** 011930
[47] Jang J S C, Li T H, Tsai P H, Huang J C and Nieh T G 2012 Critical obstacle size to deflect shear banding in Zr-based bulk metallic glass composites *Intermetallics* **64** 102–5
[48] Yang C, Cheng Q R, Liu L H, Li Y H and Li Y Y 2015 Effect of minor Cu content on microstructure and mechanical property of NiTiCu bulk alloys fabricated by crystallization of metallic glass powder *Intermetallics* **56** 37–43
[49] Hu T T, Hsu J H, Huang J C, Kuan S Y and Lee C J 2012 Correlation between reflectivity and resistivity in multi-component metallic systems *Appl. Phys. Lett.* **101** 011902
[50] Wang W H, Hsu J H and Huang J C 2013 Optical reflectivity improvement by upgrading metallic glass film quality *Appl. Phys. Lett.* **103** 161906
[51] Lin Y T, Chung Y L, Wang Z K and Huang J C 2015 AgMgAl metallic glassy and intermetallic thin films for electric contact applications *Intermetallics* **57** 133–8
[52] Lin H K, Chiu S M, Cho T P and Huang J C 2013 Improved bending fatigue behavior of flexible PET/ITO film with thin metallic glass interlayer *Mater. Lett.* **113** 182–5
[53] Lin H K, Cheng K C and Huang J C 2015 Effects of laser annealing parameters on optical and electrical properties of ITO/metallic glass alloy Bi-layer films *Nanoscale Res. Lett.* **10** 274